



**HAL**  
open science

## Origins of the extremely warm European fall of 2006

Julien Cattiaux, R. Vautard, Pascal Yiou

► **To cite this version:**

Julien Cattiaux, R. Vautard, Pascal Yiou. Origins of the extremely warm European fall of 2006. Geophysical Research Letters, 2009, 36 (6), 10.1029/2009gl037339 . hal-02346157

**HAL Id: hal-02346157**

**<https://hal.science/hal-02346157v1>**

Submitted on 28 Oct 2020

**HAL** is a multi-disciplinary open access archive for the deposit and dissemination of scientific research documents, whether they are published or not. The documents may come from teaching and research institutions in France or abroad, or from public or private research centers.

L'archive ouverte pluridisciplinaire **HAL**, est destinée au dépôt et à la diffusion de documents scientifiques de niveau recherche, publiés ou non, émanant des établissements d'enseignement et de recherche français ou étrangers, des laboratoires publics ou privés.

## Origins of the extremely warm European fall of 2006

J. Cattiaux,<sup>1</sup> R. Vautard,<sup>1</sup> and P. Yiou<sup>1</sup>

Received 16 January 2009; revised 16 February 2009; accepted 26 February 2009; published 31 March 2009.

[1] The fall of 2006 was the warmest on record in Europe. So far the origins of this seasonal extreme anomaly have not been elucidated, but understanding them is crucial since climate change may increase the frequency and amplitude of such extreme seasons. From a statistical analysis and regional modeling experiments we estimate the contributions of regional atmospheric circulation and sea-surface temperatures (SST) on the continental surface temperatures of this event. Both the regression and the dynamical model attribute about 50% of the land temperature anomaly to the atmospheric flow conditions, 30% to the SST warm anomaly, while the missing 20% remain unexplained. Assuming such decomposition, the contribution of trend components would explain about 20 to 40% of the anomaly, a proportion that should increase in the future. **Citation:** Cattiaux, J., R. Vautard, and P. Yiou (2009), Origins of the extremely warm European fall of 2006, *Geophys. Res. Lett.*, 36, L06713, doi:10.1029/2009GL037339.

### 1. Introduction

[2] The European fall and winter climate variability is mostly governed by the North-Atlantic turbulent atmospheric dynamics [Blackmon *et al.*, 1977]. The mid latitudes westerly jet stream develops strong baroclinic instabilities bringing successively polar and tropical air masses over the European continent [Charney, 1947; Wallace *et al.*, 1996]. Understanding how this variability is modified by the changes due to anthropogenic activity is a key issue to predict the evolution of European climate in the future decades. Based on an analysis of flow analogues, Yiou *et al.* [2007] showed that the European fall and winter temperature increase observed since the 1990s has become incompatible with circulation changes only. This inconsistency climaxed in the fall/winter 2006/2007 during which temperatures were significantly warmer than they would have been in the past under analogue atmospheric flow conditions [Yiou *et al.*, 2007], enhanced by factors which have not been identified so far. The fall 2006 is the warmest fall on record [Beniston, 2007; van Oldenborgh, 2007], and updated data from Xoplaki *et al.* [2005] even indicated that it was very likely the warmest fall since at least 1500 in Europe [Luterbacher *et al.*, 2007]. Such an episode had heavy impacts on the ecosystem phenology and terrestrial carbon fluxes [Luterbacher *et al.*, 2007; Piao *et al.*, 2008].

[3] The aim of this paper is to quantify the contribution of the atmospheric flow anomaly for this extreme event and to determine the impact of the extremely warm Eastern

Atlantic sea-surface temperature (SST) anomaly on the continental surface temperatures. In order to estimate these responses we used a combination of statistical methods and sensitivity experiments with a regional climate model.

### 2. Statistical Analysis of the European Fall Anomaly of 2006

[4] As shown in several previous studies [Luterbacher *et al.*, 2007; van Oldenborgh, 2007; Yiou *et al.*, 2007], the fall of 2006 (September–October–November of 2006, hereafter referred to as SON06) is the warmest fall ever recorded in Europe. The 2-meter temperature (T2m) anomaly is shown in Figure 1a from the re-analyses of the National Centers for Environmental Prediction (NCEP), which provide daily gridded data since 1948 [Kistler *et al.*, 2001]. The NCEP temperatures are strongly correlated ( $r > 0.97$  over the 1948–2007 period) with actual observations from stations of the European Climate Assessment and Data (ECA&D) project [Klein-Tank *et al.*, 2002], thus we used the NCEP data for this study. Averaged over the land areas [ $5^{\circ}\text{W}$ – $20^{\circ}\text{E}$ ;  $40^{\circ}$ – $60^{\circ}\text{N}$ ], the SON06 T2m anomaly reached  $2.6^{\circ}\text{C}$ , which corresponds to 3.5 standard deviations ( $\sigma$ ) of the 1948–2007 distribution. Although somewhat arbitrary, this area covers the main anomaly as shown in Figure 1a.

[5] This warm anomaly is linked to an unprecedented persistence of northward flow over Europe, bringing mild air from tropical Atlantic and Sahara [Luterbacher *et al.*, 2007]. The SON06 anomaly of the 500 hPa meridional wind (from NCEP) averaged over the area [ $10^{\circ}\text{W}$ – $10^{\circ}\text{E}$ ;  $40^{\circ}\text{N}$ – $60^{\circ}\text{N}$ ] is  $3.9\text{ m/s}$  ( $2.1\sigma$ ).

[6] In addition, the areas along north-western Africa, western and northern Europe are affected by a strong warm anomaly in SON06 (Figure 1c). Averaged over the “Southern” area [ $15^{\circ}\text{W}$ – $0^{\circ}$ ;  $25^{\circ}\text{N}$ – $50^{\circ}\text{N}$ ], the SON06 SST (from NCEP) is  $1.5^{\circ}\text{C}$  warmer than normal ( $3.3\sigma$ ) and the anomaly even reaches  $1.8^{\circ}\text{C}$  ( $3.6\sigma$ ) on the “Northern” area [ $10^{\circ}\text{W}$ – $15^{\circ}\text{E}$ ;  $50^{\circ}\text{N}$ – $65^{\circ}\text{N}$ ]. The “Northern” anomaly is most probably a consequence of the European warm temperature while the “Southern” anomaly may result from a deficit in the coastal upwelling of cold sea waters which usually occurs during fall in these regions (not shown). The global European SST anomaly (averaged over the “Northern” and “Southern” regions) represents  $1.6^{\circ}\text{C}$  ( $3.6\sigma$ ).

[7] As shown in Figure 1d, T2m, 500 hPa meridional wind and SST seasonal anomalies reach record values in 2006. We note that both land and sea temperatures anomalies act in a warming context (about  $0.3$ – $0.4^{\circ}\text{C}/\text{decade}$  since the 1970s [see also Xoplaki *et al.*, 2005]) while the meridional wind does not present any trend.

[8] Figure 2a shows the linear regression of daily T2m vs. meridional wind for SON 1948–2005 and SON06. The regression lines are parallel, but the SON06 line is shifted

<sup>1</sup>Laboratoire des Sciences du Climat et de l’Environnement, UMR1572, IPSL, UVSQ, CEA, CNRS, Gif-sur-Yvette, France.

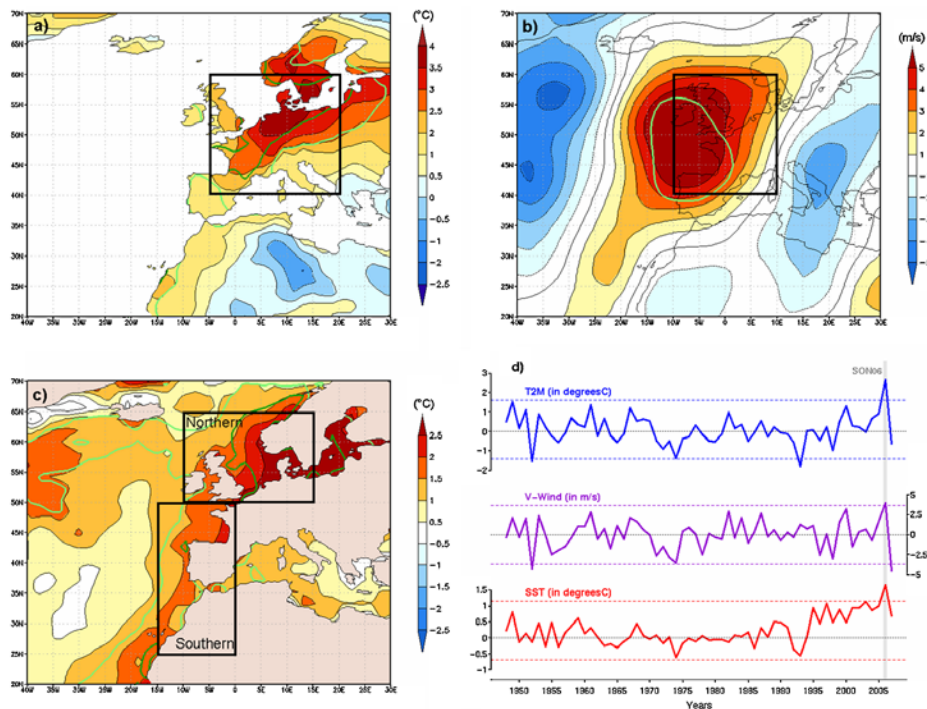


**Figure 1.** (a) NCEP SON06 anomalies of T2m, (b) meridional wind at 500 hPa, (c) SST. Green (dark green) contours correspond to  $2\sigma$  ( $3\sigma$ ) levels of the 1948–2007 distribution. (d) 1948–2007 SON time series of these variables averaged over their respective areas, indicated by black rectangles in Figures 1a–1c. The SST time series is computed by averaging over both “Northern” and “Southern” areas.

toward warmer T2m, i.e., both southward and northward flows are associated with higher temperatures than they would do in earlier years, as found by *Yiou et al.* [2007].

[9] We now investigate whether this extra warmth could be due to the Atlantic SST anomalies which remained high during the preceding falls, as suggested in [*Luterbacher et al.*, 2007]. In order to quantify the links between surface air temperature, meridional wind and SST, we compute linear regressions between their time series (Figure 2b). The correlation between actual land temperatures and those regressed from meridional wind is  $r = 0.7$  ( $p$ -value =  $8.10^{-11}$ ), confirming that the European fall temperatures strongly depend on the atmospheric flow. However the actual  $2.6^{\circ}\text{C}$  SON06 anomaly is only half reconstructed ( $1.3^{\circ}\text{C}$ ), since the meridional wind was not as extreme as the temperature during this season. More generally the regression does not reconstruct the observed warming trend observed over the past 30 years.

[10] When adding the seasonal fall SST anomalies — averaged over the both “Northern” and “Southern” oceanic regions — as a multiple linear regression predictor (Figure 2b), the correlation with the actual time series increases to  $r = 0.8$  ( $p$ -value =  $8.10^{-15}$ ). The reconstructed SON06 anomaly is now more realistic — from  $1.3^{\circ}\text{C}$  to  $2.0^{\circ}\text{C}$ , so that the contribution of the warm SST anomaly is evaluated at  $0.7^{\circ}\text{C}$  —, as well as the warming trend over the 1978–2007 period.

[11] The multiple regression model does not explain all anomalies such as the 1993 very cold peak. In order to fully

understand the physics of the SON06 anomaly modeling experiments are necessary.

### 3. Modeling Experiments

[12] We use the Penn State University - National Center for Atmospheric Research fifth generation mesoscale model (MM5) [*Dudhia*, 1993; *Grell et al.*, 1994], with the same set of physical parameterizations and the same land-surface model as *Salameh et al.* [2009]. The domain considered covers the Eastern Atlantic – Western Europe area [ $40^{\circ}\text{W}$ – $30^{\circ}\text{E}$ ;  $20^{\circ}$ – $67^{\circ}\text{N}$ ] and is composed of  $150 \times 150$  grid points, with a horizontal resolution increasing with the latitude (from  $\sim 51$  km at  $20^{\circ}\text{N}$  to  $\sim 21$  km at  $67^{\circ}\text{N}$ ). Simulations are initialized on August 31, 2006 at 18:00 UT, allowing 6 hours of spin-up time, and driven with boundary conditions from the operational analyses from the European Centre for Medium Range Weather Forecast (ECMWF) all along SON06. We performed some of the sensitivity experiments by nudging the wind 3D field by the ECMWF field, but in order not to influence thermodynamical fields, no nudging is applied to temperature and humidity 3D fields.

[13] A control simulation (referred to as CTL) is performed with the SON06 actual SST conditions (taken from NCEP 4 times daily re-analyses), and wind nudging. A sensitivity simulation is computed using SSTs from the 4 times daily SON 1961–1990 climatology instead of the actual SON06 ones, and still nudging the wind (hereafter referred to as WNC, for “Wind Nudged – Climatological

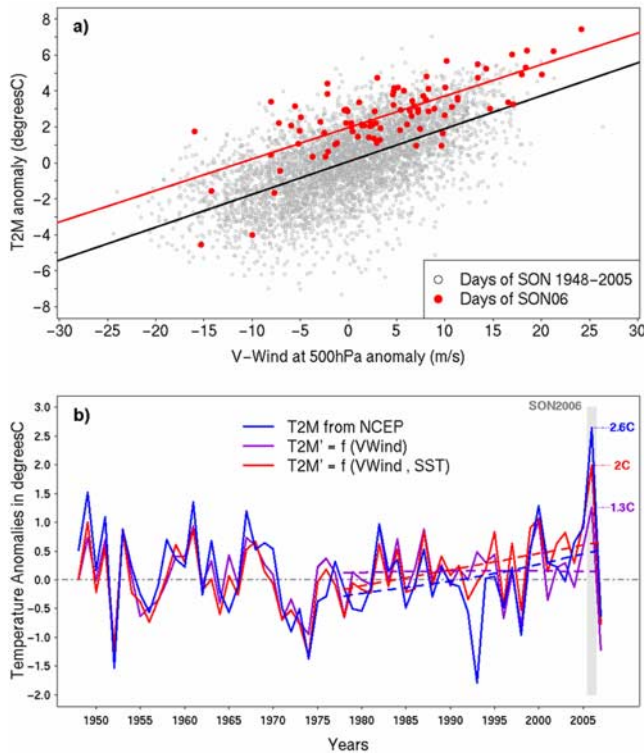


**Figure 2.** (a) Correlation between daily regional anomalies of T2m and meridional wind for all days of fall 1948–2006. Days of 1948–2005 (2006) are shown in gray (red). Linear regressions are added in respective colors. (b) Reconstruction of the fall T2m anomaly (blue) from the fall meridian wind anomaly only (purple) and from the fall meridian wind anomaly + the fall SST anomaly (red) over the 1948–2007 period. The 1978–2007 trends are added in dashed lines.

SSTs”). WNC and CTL therefore have very close atmospheric circulation conditions. The temperature difference between the two experiments gives the direct response to the SON06 SST anomaly.

[14] We perform a second sensitivity simulation (hereafter referred to as the WFC simulation, for “Wind Free – Climatological SSTs”), with climatological SSTs, but no wind nudging. The difference between WFC and CTL is expected to give the combined effect of SON06 SST and circulation anomalies, while the difference between WFC and WNC gives the contribution of the atmospheric circulation in standard SST conditions. Following this methodology, the circulation contribution is probably incompletely identified since all simulations are forced at the boundaries by the same analyzed ECMWF flow. The regional flow obtained here by relaxing the nudging constraint is one possible realization, but may not be representative of “average flows”. This has to be kept in mind in the following for all interpretations concerning the flow effects.

[15] The model is first evaluated by comparing the CTL simulation with averaged T2m from NCEP (Figure 3). As shown in previous work the MM5 model is known to have a homogeneous cold bias of about  $-0.5$  to  $-1^{\circ}\text{C}$  over Europe

[Giorgi *et al.*, 2004; Kotlarski *et al.*, 2005]. In order to estimate the spatial skill of the model, we compute a bootstrap test on the number of grid points used to average regionally, giving a 95% confidence interval (indicated between brackets) for each regional mean [von Storch and Zwiers, 2001]. Thus we find a bias of  $-1.2^{\circ}\text{C}$  ( $-1.0/-1.3^{\circ}\text{C}$ ) relative to the NCEP daily averages interpolated on the MM5 grid over the  $[5^{\circ}\text{W}-20^{\circ}\text{E}; 40-60^{\circ}\text{N}]$  continental area (Figure 3a), which is stronger in coastal areas (Atlantic and Mediterranean – Figure 3b). The model also has a warm bias over Northern Africa. However the SON06 variability is well represented by our model, since the correlation between the CTL and NCEP time series is about  $r = 0.9$  over the whole domain (Figure 3c).

[16] By subtracting WNC from CTL we find that the contribution of the SON06 SST anomaly (Figure 1c) to the land surface temperature anomaly is temporally (Figure 3a) and spatially (Figure 4b) homogeneous. Over the  $[5^{\circ}\text{W}-20^{\circ}\text{E}; 40-60^{\circ}\text{N}]$  land areas, the mean temperature difference is  $0.8^{\circ}\text{C}$  ( $\pm 0.05^{\circ}\text{C}$ ), which is consistent with the  $0.7^{\circ}\text{C}$  found with the statistical regression models.

[17] In order to better estimate the SST anomaly contribution, we performed two more experiments. First, by dividing the SST anomaly above and below  $50^{\circ}\text{N}$ , we observed that the effects on continental temperatures are additive: the Northern (Southern) SST anomaly leads to a global warming of the Northern (Southern) continental Europe (not shown). Thus, the “mean upwind” part of the anomaly is not more influential than its “mean downwind” part, probably because instantaneous flows spread the anomaly in an efficient manner. Then we evaluated the contribution of the part of the SST anomaly linked to the long-term warming trend by performing a simulation using Wind Nudging and Current Climatological (WNCC) SSTs (from the 1996–2005 mean). The responses to both trend part (WNCC-WNC difference) and extra warmth (CTL-WNCC difference) of the SON06 anomaly are similar:  $0.4^{\circ}\text{C}$  ( $\pm 0.03^{\circ}\text{C}$ ).

[18] Without wind nudging (WFC), the meridional flow at 500 hPa remains mostly northward (because of the boundary conditions of SON06), but with a 2.8 m/s weaker amplitude than the CTL wind over the  $[10^{\circ}\text{W}-10^{\circ}\text{E}; 40-60^{\circ}\text{N}]$  region. The spatial structure of the difference (Figure 4a) resembles the SON06 meridional wind anomaly from NCEP (Figure 1b), even though the pattern is slightly shifted north-eastward. The mean WFC land surface temperature is cooler than the CTL one by  $1.6^{\circ}\text{C}$  ( $1.5/1.8^{\circ}\text{C}$ ) over the  $[5^{\circ}\text{W}-2^{\circ}\text{E}; 40-60^{\circ}\text{N}]$  land areas, with a spatial difference which is similar, albeit weaker, to the SON06 NCEP anomaly (Figures 4c and 1a). The time variations of temperatures along the season differ (Figure 3), due to the difference of instantaneous atmospheric circulation.

[19] The meridional wind effect is isolated by subtracting WFC to WNC, which induces a 2.8 m/s mean meridional wind difference over the  $[10^{\circ}\text{W}-10^{\circ}\text{E}; 40-60^{\circ}\text{N}]$  region and a  $0.9^{\circ}\text{C}$  ( $0.7/1.1^{\circ}\text{C}$ ) mean land surface temperature difference over the  $[5^{\circ}\text{W}-2^{\circ}\text{E}; 40-60^{\circ}\text{N}]$  land areas (Figures 4a and 4d). Extrapolating to the actual SON06 meridional wind anomaly (3.9 m/s) with the same wind/temperature ratio would lead to a  $1.3^{\circ}\text{C}$  ( $1.0/1.5^{\circ}\text{C}$ )



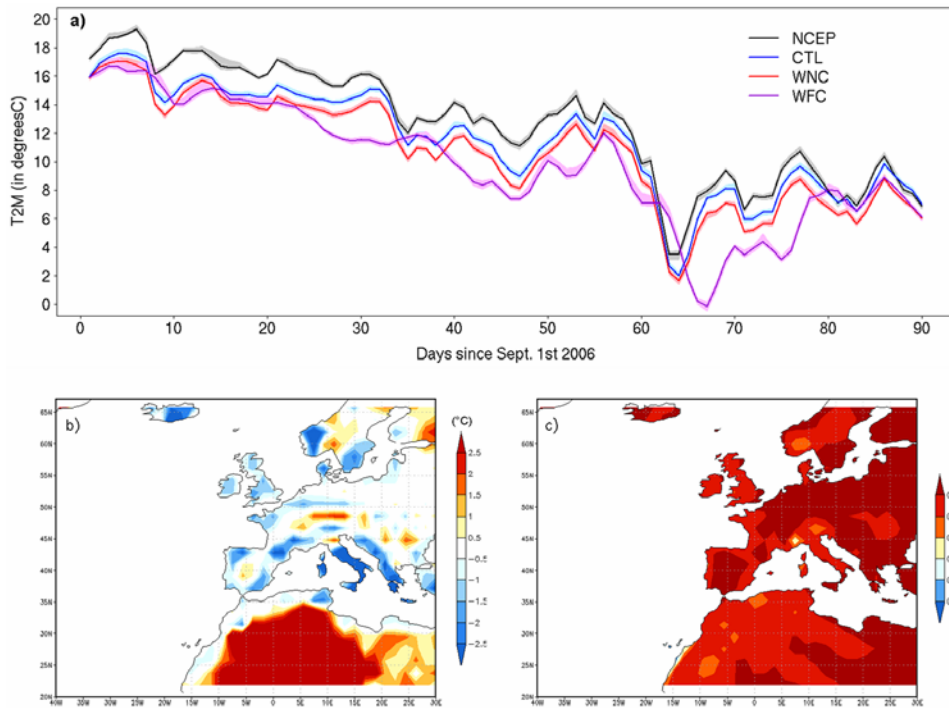


**Figure 3.** (a) Comparison between daily T2m of MM5-CTL (blue), MM5-WNC (red), MM5-WFC (purple) and NCEP (black) over SON06 days, averaged over the land area (5°W–20°E; 40–60°N). 95% confidence intervals are added in shaded areas. (b) Mean SON06 T2m difference between MM5-CTL and NCEP. (c) Correlation between SON06 daily time series of MM5-CTL and NCEP, on each grid point of the NCEP grid.

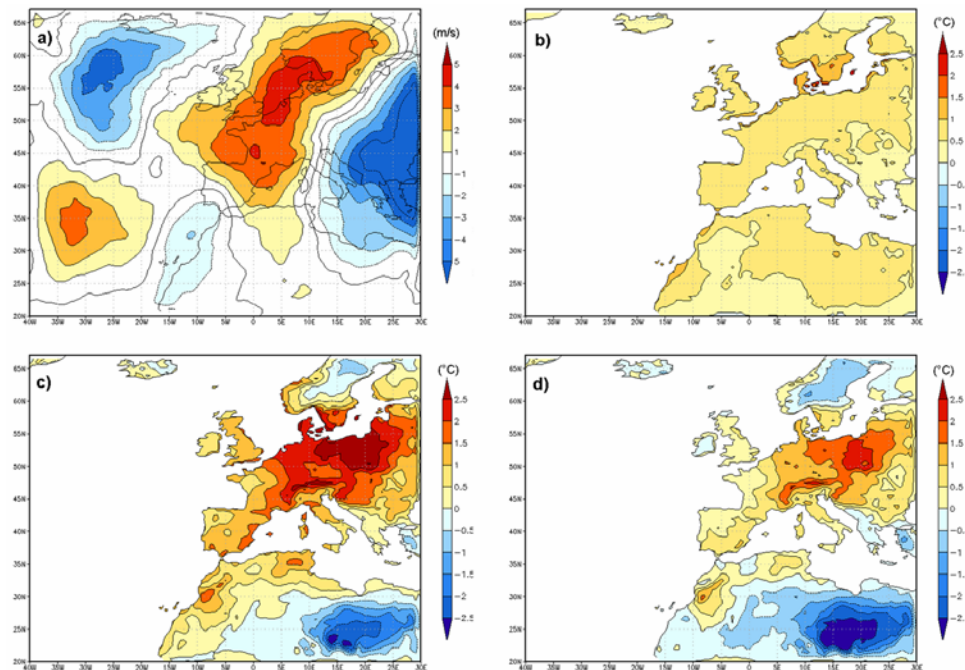


**Figure 4.** Mean SON06 MM5 simulations differences of (a) meridional wind at 500hPa between CTL/WNC and WFC, and T2m between (b) CTL and WNC, (c) CTL and WFC, (d) WNC and WFC.

temperature difference, as predicted by the regression model (Figure 2b).

#### 4. Discussion

[20] Both statistical and dynamical methods attribute about 50% (1.3°C over 2.6°C) of the SON06 T2m anomaly to the atmospheric flow anomaly and about 30% (0.7/0.8°C over 2.6°C) to the SST one.

[21] The additivity between the two responses is surprising because the two forcings are not independent. At least part of the SST anomalies could be due to the circulation anomaly itself: the increased eastward wind along North-African coasts reduces the upwelling and the northward flow across Europe increases SST in the North and Baltic Seas. The statistical model implicitly takes these SST feedbacks in the wind regression model while the dynamical approach underestimates the full circulation response. The atmospheric circulation anomaly also induces local feedbacks like the strong increase of short-wave radiation in Central-Eastern Europe (more than 20 W/m<sup>2</sup> in some areas, not shown), where more anticyclonic weather develops. Such feedbacks may also induce nonlinear effects perturbing our linear estimation of contributions. In order to draw more general conclusions about linearity of responses the analysis of other seasons is planned, but left for future studies.

[22] Other SST anomalies in other parts of the world, for instance in the Pacific region, may have contributed to the fall 2006 warm anomaly. However such remote origins are supposed to be mostly contained in the circulation anomalies since they are known to propagate to the extra-tropics through Rossby wave trains [Cassou, 2008].

[23] Another important question is the attribution of the man-induced contribution to this anomaly. While this question can in principle only be tackled in terms of risks of extremes [Stott et al., 2004], a rough estimate of this contribution can be given under the simplistic assumption that the man-induced contribution lies only in model-domain (Eastern Atlantic) SST and boundary-conditions. The former contribution is 0.4°C while the latter has not been formally estimated but should be part of the unexplained 20% of the T2m anomaly (0.5/0.6°C). Thus the man-induced contribution to the SON06 anomaly is estimated between 0.4°C and 1.0°C (20–40% of the anomaly). This proportion should increase under enhanced radiative forcing as expected in the 21<sup>st</sup> century, suggesting that more and more warm events could appear and develop during fall seasons in the future [Beniston, 2007; Scherrer et al., 2007].

#### 5. Conclusions

[24] We have used a statistical and a dynamical model to analyze the fall 2006 temperature anomaly over Europe. The anomalous atmospheric flow and SST have significant contributions to temperature variations, which explain overall about 80% (2.0/2.1°C) of the 2.6°C temperature anomaly of SON06. The atmospheric circulation influences the spatial and temporal variability while the warm SSTs globally shift the land temperatures towards higher values. The remaining 20% of the anomaly (0.5/0.6°C) may be due to other processes, nonlinearity, or to anomalous background temperatures and global flow configuration during

SON06 [Luterbacher et al., 2007; van Oldenborgh, 2007]. Since the warming trend of the Atlantic SSTs does not seem to slow down, our results suggest that the probability of such a warm event over Europe will increase in the future.

[25] **Acknowledgments.** We thank the anonymous reviewers for useful comments. This work was partly supported by the French ANR CHAMPION project.

#### References

- Beniston, M. (2007), Entering into the “greenhouse century”: Recent record temperatures in Switzerland are comparable to the upper temperature quantiles in a greenhouse climate, *Geophys. Res. Lett.*, *34*, L16710, doi:10.1029/2007GL030144.
- Blackmon, M. L., et al. (1977), An observational study of the Northern Hemisphere wintertime circulation, *J. Atmos. Sci.*, *7*, 1040–1053, doi:10.1175/1520-0469.
- Cassou, C. (2008), Intraseasonal interaction between the Madden-Julian Oscillation and the North Atlantic Oscillation, *Nature*, *455*, 523–527, doi:10.1038/nature07286.
- Charney, J. G. (1947), The dynamics of long waves in a baroclinic westerly current, *J. Atmos. Sci.*, *5*, 136–162, doi:10.1175/1520-0469.
- Dudhia, J. (1993), A nonhydrostatic version of the Penn State–NCAR Mesoscale Model: Validation tests and simulation of an Atlantic cyclone and cold front, *Mon. Weather Rev.*, *5*, 1493–1513, doi:10.1175/1520-0493.
- Giorgi, F., X. Bi, and J. S. Pal (2004), Mean, interannual variability and trends in a regional climate change experiment over Europe. I. Present-day climate (1961–1990), *Clim. Dyn.*, *6*, 733–756, doi:10.1007/s00382-004-0409-x.
- Grell, G. A., J. Dudhia, and D. R. Stauffer (1994), A Description of the Fifth-Generation Penn State/NCAR Mesoscale Model (MM5), *NCAR Tech. Note NCAR/TN-398 + STR*, Natl. Cent. for Atmos. Res., Boulder, Colo.
- Kistler, R., et al. (2001), The NCEP/NCAR 50-year reanalysis: Monthly means, *Bull. Am. Meteorol. Soc.*, *82*, 247–267.
- Klein-Tank, A., et al. (2002), Daily dataset of 20th-century surface air temperature and precipitation series for the European Climate Assessment, *Int. J. Climatol.*, *22*, 1441–1453, doi:10.1002/joc.773.
- Kotlarski, S., et al. (2005), Regional climate model simulations as input for hydrological applications: Evaluation of uncertainties, *Adv. Geosci.*, *5*, 119–125.
- Luterbacher, J., M. A. Liniger, A. Menzel, N. Estrella, P. M. Della-Marta, C. Pfister, T. Rutishauser, and E. Xoplaki (2007), Exceptional European warmth of autumn 2006 and winter 2007: Historical context, the underlying dynamics, and its phenological impacts, *Geophys. Res. Lett.*, *34*, L12704, doi:10.1029/2007GL029951.
- Piao, S., et al. (2008), Net carbon dioxide losses of northern ecosystems in response to autumn warming, *Nature*, *451*, 49–52, doi:10.1038/nature06444.
- Salameh, T., P. Drobinski, and T. Dubos (2009), The effect of indiscriminate nudging time on the large and small scales in regional climate modelling: Application to the Mediterranean basin, *Q. J. R. Meteorol. Soc.*, in press.
- Scherrer, S. C., C. Appenzeller, and M. A. Liniger (2007), Distribution changes of seasonal mean temperature in observations and climate change scenarios, in *Climate Variability and Extremes During the Past 100 Years*, *Adv. Global Change Res. Book Ser.*, vol. 33, edited by S. Broennimann et al., pp. 251–267, Springer, New York.
- Stott, P., D. A. Stone, and M. Allen (2004), Human contribution to the European heatwave of 2003, *Nature*, *432*, 610–614, doi:10.1038/nature03089.
- van Oldenborgh, G. J. (2007), How unusual was autumn 2006 in Europe?, *Clim. Past*, *3*, 659–668.
- von Storch, H., and F. W. Zwiers (2001), *Statistical Analysis in Climate Research*, Cambridge Univ. Press, Cambridge, U. K.
- Wallace, J. M., Y. Zhang, and L. Bajuk (1996), Interpretation of interdecadal trends in Northern Hemisphere surface air temperature, *J. Clim.*, *2*, 249–259, doi:10.1175/1520-0442.
- Xoplaki, E., J. Luterbacher, H. Paeth, D. Dietrich, N. Steiner, M. Grosjean, and H. Wanner (2005), European spring and autumn temperature variability and change of extremes over the last half millennium, *Geophys. Res. Lett.*, *32*, L15713, doi:10.1029/2005GL023424.
- Yiou, P., R. Vautard, P. Naveau, and C. Cassou (2007), Inconsistency between atmospheric dynamics and temperatures during the exceptional 2006/2007 fall/winter and recent warming in Europe, *Geophys. Res. Lett.*, *34*, L21808, doi:10.1029/2007GL031981.

J. Cattiaux, R. Vautard, and P. Yiou, Laboratoire des Sciences du Climat et de l'Environnement, UMR1572, IPSL, UVSQ, CEA, CNRS, F-91191 Gif-sur-Yvette CEDEX, France. (julien.cattiaux@lscce.ipsl.fr)